

Study and Numerical Simulation of Negative and Positive Corona Discharge: A Review

Angel Asipuela^{1*}, Tamás Iváncsy¹

¹ Department of Electric Power Engineering, Faculty of Electrical Engineering and Informatics, Budapest University of Technology and Economics, H-1521 Budapest, P.O.B. 91, Hungary

* Corresponding author, e-mail: gabriel.bme_2020@edu.bme.hu

Received: 01 February 2022, Accepted: 19 April 2022, Published online: 31 May 2022

Abstract

Two models to describe the phenomenon of corona discharge are presented: the first is known as the plasma model which with plasma chemistry defines the volumetric and surface reactions among charge carriers such as electrons, positive, and negative ions. This model uses Poisson's equation and a formulation of the space-charge density to calculate the electric field necessary to solve the species transport equations. Besides, only the plasma model determines the density of the charge carriers. The second is a simplified model which describes the corona discharge in terms of current conservation coupled with Poisson's equation. This model does not have any connection with the attributes of plasma chemistry. Both models propose solutions for the electric potential and space charge density distribution from the corona electrode to the ground electrode.

Keywords

corona discharge, ESP, electron transport, plasma in corona, charge density

1 Introduction

In industrial applications ESPs (Electrostatic precipitators) use a negative corona because of its better performance, as an example, Cottrell showed based on experimental work to have much better results using a negative corona than a positive corona [1]. As part of this study, two types of corona are described and modeled.

The corona discharge can be described by two different models, the first is a full self-consistent plasma model and the second is a simplified model. "*The plasma model solves the electron and ion continuity and momentum equations in the drift-diffusion approximation, self-consistently coupled with Poisson's equation*" [2]. In the case of the simplified model, it is based on the current conservation and electric field established in the corona wire, which determines the space charge density and electric field [2].

For the plasma model, the coefficients needed to calculate the electron density and the electron energy can be computed by distribution functions or using Boltzmann's equation. Using Boltzmann's equation requires a lot of effort which is why a simplified model of that equation is used. The electron transport is defined by the drift-diffusion equation and the transport of heavy species is defined by another different transport equation, where the diffusive

flux vector can be defined according to a Mixture averaged or Flick's law diffusion model. Additionally, in the plasma model, the electrostatics is governed by Poisson's equation, and the space charge density is computed directly by an equation defined in the plasma chemistry. The boundary conditions are defined based on the charge carrier behavior, for instance, the electrons on the walls are lost or gained if they are affected by the secondary emission effects, these conditions are expressed by the normal of the flux vector. In the case of non-electron species, the ions are lost to the walls, and the boundary condition can be defined as the normal component of the diffusive flux vector. In plasma chemistry, the species need to be specified, in general, cold plasma has many reactions, however, for simplicity only certain reactions are considered for the model. It should also be considered that there are volumetric reactions and surface reactions. The reactions among electrons, positive ions, negative ions, and neutral species are considered volumetric reactions. And in the case of surfaces reactions happen when these volumetric bodies collide with the surfaces of the walls.

For the simplified model, there is no plasma chemistry definition, it uses the charge conservation equation

coupled with Poisson's equation, for this model the potential and electric field need to be defined at the corona electrode, for instance, the electric field onset is computed by Peek's law.

Finally, according to the plasma model, the electron density, positive, and negative ion density are computed along with the space between the corona electrode and ground electrode, and then the results obtained are illustrated in the corresponding section. In addition, for both models, the electric potential and space charge density are shown in the results section.

2 Physical model

2.1 Plasma model

In this model, the behavior of charged species (electrons, negative and positive ions) is described by fluid-type equations. It will simulate the ionization of neutral gas and the transport of charged particles. It should be considered that the corona discharge is diffuse and uniform in the discharge space [2].

The coefficients needed to compute the electron density and electron energy are obtained from collision-section data and electron energy distribution function (EEDF). EEDF can be defined by Maxwellian, Druyvesteyn, and Generalized distribution functions or explicitly calculated using Boltzmann's equation, with the two-term approximation [3].

The EEDF can be defined by Eq. (1) in the case of Maxwellian $g = 1$, Druyvesteyn $g = 2$, and Generalized distribution function $1 < g < 2$.

$$f(\varepsilon) = g\varphi^{-3/2}\beta_1 \exp\left(-(\varepsilon\beta_2/\varphi)^g\right) \quad (1)$$

$$\beta_1 = \Gamma(5/2g)^{3/2} \Gamma(3/2g)^{-5/2}$$

$$\beta_2 = \Gamma(5/2g)\Gamma(3/2g)^{-1}$$

f is the electron distribution function, ε is the electron energy, φ is the mean electron energy, and Γ is the upper incomplete gamma function.

EEDF also can be computed by Boltzmann's Eq. (2), which is a nonlocal continuity equation in the six-dimensional phase space (\mathbf{r} , \mathbf{v}) of particle positions and velocities [3, 4].

$$\frac{\partial f}{\partial t} + \mathbf{v} \cdot \nabla f - \frac{e\mathbf{E}}{m_e} \cdot \nabla_v f = \frac{\partial f}{\partial t} \Big|_c \quad (2)$$

Because of the complexity of solving this equation in terms of computation, Boltzmann's equation has been simplified for a two-terms approximation [5]. This

approximation is valid for the values obtained from the reduced electric field and the equation for f looks like a convection-diffusion continuity-equation in energy space [3, 5].

$$\frac{\partial}{\partial \varepsilon} \left(Wf - D \frac{\partial f}{\partial \varepsilon} \right) = S \quad (3)$$

W and D are calculated based on the properties of the electrons and the background gas, and S is the source term representing the energy loss because of inelastic collisions [3]. Generally, electron transport is described by Boltzmann's equation.

2.1.1 Electron transport

The electron density can be solved by the drift-diffusion equation, see Eq. (4), this equation does not introduce the photoionization effect [6]:

$$\frac{\partial}{\partial t} (n_e) + \nabla \cdot \Gamma_e = R_e - (\mathbf{u} \cdot \nabla) n_e, \quad (4)$$

$$\Gamma_e = -(\mu_e \cdot \mathbf{E}) n_e - \nabla \cdot (\mathbf{D}_e n_e). \quad (5)$$

n_e (1/m³) is the electron density, Γ_e (1/(m²s)) is the electron flux vector, R_e is the electron source due to chemical reactions [7], \mathbf{u} is the neutral fluid velocity vector, μ_e (m²/Vs) is the electron mobility, \mathbf{E} (V/m) is the electric field, and \mathbf{D}_e (m²/s) is the electron diffusivity, computed by $\mathbf{D}_e = \mu_e T_e$, and T_e (V) is the electron temperature [2, 5, 8, 9]. The electron energy density is described by:

$$\frac{\partial}{\partial t} (n_\varepsilon) + \nabla \cdot \Gamma_\varepsilon + \mathbf{E} \cdot \Gamma_e = S_{en}, \quad (6)$$

$$\Gamma_\varepsilon = -(\mu_\varepsilon \cdot \mathbf{E}) n_\varepsilon - \nabla \cdot (\mathbf{D}_\varepsilon n_\varepsilon), \quad (7)$$

where n_ε (V/m³) is the electron energy density; Γ_ε (V/(m²s)) is the electron energy flux vector; S_{en} (V/(m³s)) is the energy loss/gain due to inelastic collisions [7]; $\mu_\varepsilon = 5/3 \cdot \mu_e$ (m²/Vs) is the electron energy mobility; and $\mathbf{D}_\varepsilon = 5/3 \cdot \mathbf{D}_e$ (m²/s) is the electron energy diffusivity [10]. By a local field approximation, the relation between the mean electron energy and the reduced electric field is defined, see Eq. (8):

$$\varepsilon = F(E/N_n). \quad (8)$$

E/N_n is the reduced electric field, E is the electric field, and N_n is the density of the background gas.

Eq. (9) represents the electron source, where its coefficients are defined by plasma chemistry:

$$R_e = \sum_{j=1}^M x_j k_j N_n n_e. \quad (9)$$

M is the number of reactions, and P is the number of inelastic electron-neutral collisions, P is much higher than M , x_j is the mole fraction of the target reaction, k_j (m³/s) is the rate coefficient, and N_n (1/m³) is the total neutral number density [3, 8]. In the case of DC discharges is better to use Townsend coefficients, where the electron source equation is expressed as follows:

$$R_e = \sum_{j=1}^M x_j \alpha_j N_n |\Gamma_e|. \quad (10)$$

α_j (m²) is the Townsend coefficient for the reaction [3, 8].

2.1.2 Heavy species transport

For modeling mass transport, Maxwell-Stefan equations are the only one that conserves the total mass in a system, however, the number of computational resources is the main drawback. Therefore, two diffusion models less computational are approached: Mixture averaged and Flick's law [3].

In the case of non-electron species, the transport equation is defined as Eq. (11):

$$\rho \frac{\partial}{\partial t} (w_k) + \rho (\mathbf{u} \cdot \nabla) w_k = \nabla \cdot \mathbf{j}_k + R_k. \quad (11)$$

ρ (kg/m³) is the density of the mixture, w_k is the mass fraction, \mathbf{u} (m/s) is the mass-averaged fluid velocity vector, $\mathbf{j}_k = \rho w_k \mathbf{V}_k$ is the diffusive flux vector, R_k (kg/m³s) is the rate expression for species k [3], and \mathbf{V}_k is the multicomponent diffusion velocity for species k and its formulation changes if Mixture Averaged or Flick's law is chosen.

2.1.3 Electrostatics

The electrostatic phenomena can be described by Poisson's equation, see Eq. (12).

$$\varepsilon_0 \varepsilon_r \cdot \nabla^2 V = -\rho_q \quad (12)$$

$$\mathbf{E} = -\nabla V \quad (13)$$

ε_0 is the vacuum permittivity, V is the electric potential, and ρ_q (C/m³) is the space charge density.

Based on the plasma chemistry model, the following equation computes the space charge density [3, 8]:

$$\rho_q = q \left(\sum_{k=1}^N Z_k n_k - n_e \right), \quad (14)$$

where q is the elementary charge, Z_k is the number of charges taken for a k -element, and n_k is the density of a k -element.

2.1.4 Boundary conditions

The electrons are lost to the wall due to random motion and gained because of the secondary emission effects. The boundary conditions for the electron flux and the electron energy flux are defined by Eq. (15) and Eq. (16) respectively [3].

$$\mathbf{n} \cdot \Gamma_e = \frac{1-r_e}{1+r_e} \left(\frac{1}{2} v_{e,th} n_e \right) - \left[\sum_p \gamma_p (\Gamma_p \cdot \mathbf{n} + \Gamma_t \cdot \mathbf{n}) \right] \quad (15)$$

$$\mathbf{n} \cdot \Gamma_\varepsilon = \frac{1-r_e}{1+r_e} \left(\frac{5}{6} v_{e,th} n_e \right) - \left[\sum_p \gamma_p \bar{\varepsilon}_p (\Gamma_p \cdot \mathbf{n} + \bar{\varepsilon}_t \Gamma_t \cdot \mathbf{n}) \right] \quad (16)$$

\mathbf{n} is the normal component, r_e is the reflection coefficient, $v_{e,th}$ (m/s) is the thermal velocity, see Eq. (17), is the secondary emission coefficient, γ_p is the thermal emission flux, $\bar{\varepsilon}_p$ (V) is the mean energy of p -species of the secondary electrons, and $\bar{\varepsilon}_t$ (V) is the mean energy of thermally emitted electrons.

$$v_{e,th} = \sqrt{\frac{8k_b T_e}{\pi m_e}} \quad (17)$$

The insulation boundary conditions for electron and electron energy flux are set to zero, $\mathbf{n} \cdot \Gamma_e = 0$, $\mathbf{n} \cdot \Gamma_\varepsilon = 0$.

In the case of heavy species, the ions are lost to the wall, then this condition is described as follows:

$$\mathbf{n} \cdot \mathbf{j}_k = M_w R_k + M_w c_k Z \mu_k (\mathbf{E} \cdot \mathbf{n}) [Z_k \mu_k (\mathbf{E} \cdot \mathbf{n}) > 0]. \quad (18)$$

M_w (kg/(mol)) is the molecular weight, R_k is the rate expression of species k determined by the stoichiometry of the system, c_k (mol/m³) is the molar concentration of species k , and μ_k is the mobility of species k [3].

2.1.5 Plasma chemistry

The air chemistry can be represented by a set of charged and no-charged species, namely e, O, O₂, O₃, N₂⁺, N₄⁺, O₂⁺, O₄⁺, O₂⁺N₂, O₂⁻, O⁻ and N₂ [6]. About 15 to 27 reactions have been used to represent certain models [9, 11]. However, the focus of this work is to consider the study of charge particle density and currents, therefore, a simplified set of reactions is defined, which helps to describe the creation and destruction of charged species [3]. For the fluid equations, the gas is composed of a general species denoted as A , which can form positive and negative ions.

The established collisions and reactions are shown in Table 1.

In Table 1 e denotes an electron, p is a neutral species, i is a positive ion, n is a negative ion. Moreover, when the

Table 1 Plasma chemistry, volumetric collisions, and reactions [3]

Reaction	Formula	Type
1	$e + A \rightarrow p + 2e$	ionization
2	$e + A \rightarrow n$	attachment
3	$e + 2A \rightarrow n + A$	three-body attachment
4	$e + p \rightarrow A$	e-p recombination
5	$n + p \rightarrow 2A$	n-p recombination

ions collide with the wall, they become neutral atoms. That is the case of surface reactions, where $p \rightarrow A$ and $n \rightarrow A$.

2.2 Simplified model

This model is based on the conservation of current transported by the charge carriers, it solves the transport of a charge carrier using the charge conservation equation coupled with Poisson's equation, see Eq. (12). Besides, it is not a self-consistent model, therefore, the potential and electric field should be given at the corona wire [2].

$$\nabla \cdot \mathbf{J} = S \quad (19)$$

$$\mathbf{J} = z_q \mu \rho_q \mathbf{E} \quad (20)$$

\mathbf{J} (A/m²) is the current density, S (A/m³) is a current source, z_q is the charge number, and μ (m²/Vs) is mobility.

Combining the Poisson's and the charge conservation equations, the transport equation can be defined as follows:

$$\mu \left(\frac{\rho_q^2}{\epsilon_0} - \nabla V \cdot \nabla \rho_q \right) = S. \quad (21)$$

Neglecting the diffusion current, Eq. (21) can be expressed as Eq. (22) which is widely used, denoting that there is no connection with the attributes of the plasma definition [2].

$$\frac{\rho_q^2}{\epsilon_0} - \nabla V \cdot \nabla \rho_q = 0 \quad (22)$$

2.2.1 Boundary conditions

The first condition to solve in Poisson's equation is given by the normal of the electric field, described by Eq. (23):

$$\mathbf{n} \cdot \mathbf{E} = E_0, \quad (23)$$

where E_0 (V/m) is the onset electric field computed by experimental work established by Peek's law [2]. According to Peek's equation, the onset electric field E_0 (V/m) is defined by δ which is the relation between temperature and pressure, and the radius of the corona wire r_0 (m) [1, 12].

$$E_0 = 3 \cdot 10^6 \delta \left(1 + 0.03 / \sqrt{\delta r_0} \right) \quad (24)$$

$$\delta = \frac{T_0}{T} \cdot \frac{P}{P_0} \quad (25)$$

T_0 (293.15 °K) is the absolute temperature, P_0 (760 mmHg) is the normal atmospheric pressure, P and T are the actual-operating values. The second condition is $V = 0$ (V) at the collecting plates, and there are no electronic charges at the inlet and outlet. In the transport equation, Eq. (21), ρ_q needs to be defined at the corona electrode, the condition is defined using a Lagrange multiplier, that verifies the imposed voltage V_0 if $V - V_0 = 0$ [2].

3 Corona discharge simulation

3.1 Software setting

With the help of software tools, the corona discharge effect can be estimated, allowing the number of electrons and charge carriers to be quantified. There are also methods through programming language to estimate the charge carriers by solving the differential equations, such as the proposed study of radio-frequency plasma simulation [13]. However, due to the software facilities, we will limit ourselves to obtaining the proposed results through COMSOL Multiphysics to simulate the models described in this paper. In this work, a specific case study is performed, and the geometric parameters of ESP [14, 15], together with the operating conditions presented in Table 2. Besides, there are other parameters to be specified to carry out the simulation such as ion mobility, recombination, gas pressure and temperature, initial conditions for the density of electrons and ions, and the applied voltage.

The first part to be defined is the plasma model part, which includes the displacement current equation; the relation between the mean electron energy and the reduced electric field; and the drift-diffusion equation. For the transport equation, a Mixture-averaged diffusion model is selected, the mean electron energy is defined by a local field approximation, and EEDF is defined by a Maxwellian distribution function [7]. In the case of

Table 2 Specific geometry for the ESP arrangement

Description	Value
Electrode radius (mm)	0.5
Distance between the collecting plates (mm)	65
Applied voltage (kV)	20
Material	Air
Gas temperature (°K)	293.15
Gas pressure (mmHg)	760

the species, A is described as a neutral species, e is an electron, p is a positive ion with $z = 1$, and n is a negative ion with $z = -1$. Based on the above, the volumetric collisions and reactions are established as follows, three kinds of volumetric collisions: the first collision type is the ionization, ($e + A \rightarrow p + 2e$), with an energy loss of 15 V, and the rate constant is given by Townsend coefficient; the second is an attachment type, ($e + A \rightarrow n$), where the rate constant is given by Townsend coefficient, and the third is also an attachment type with the formulation ($e + A + A \rightarrow n + A$). Two volumetric recombination-type reactions: ($e + p \rightarrow A$) and ($n + p \rightarrow A + A$). Lastly, three surface reactions: the first ($p \rightarrow A$) is placed at the corona electrode, where the secondary reaction parameters are specified, the second ($p \rightarrow A$) is placed at the ground electrode, and the third ($n \rightarrow A$) is placed at both electrodes. The plasma model is mainly defined by the drift-diffusion equation and Poisson's equation, where the temperature and pressure should be specified, and the relation between the reduced electric field and the mean electron energy need to be provided. The second part is the electrostatics component, Poisson's equation is defined for the charge conservation. The third part is the charge transport component, where the charge conservation is defined by Eq. (20). When all the settings are established with the plasma model, the positive and negative corona are simulated by a time-dependent study case. For the simplified model, the positive and negative corona is conducted by a stationary study case.

4 Results and discussion

Fig. 1 and Fig. 2 show the distribution of charge carriers, both for the positive and negative corona respectively.

In the case of a positive corona (see Fig. 1), a rapid decrease of the electrons is observed, it does not prevail very far from the electrode corona, a high number

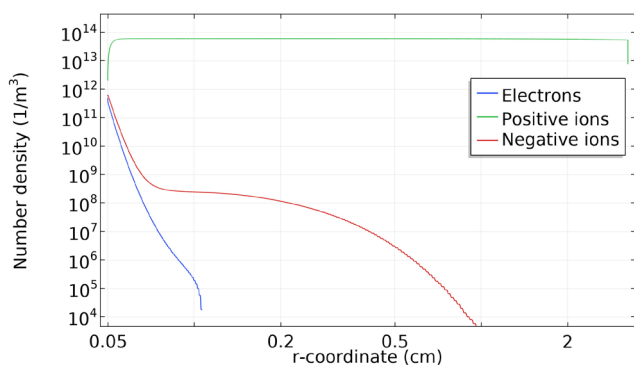


Fig. 1 Positive corona - Charge carriers in logarithmic scale [4]

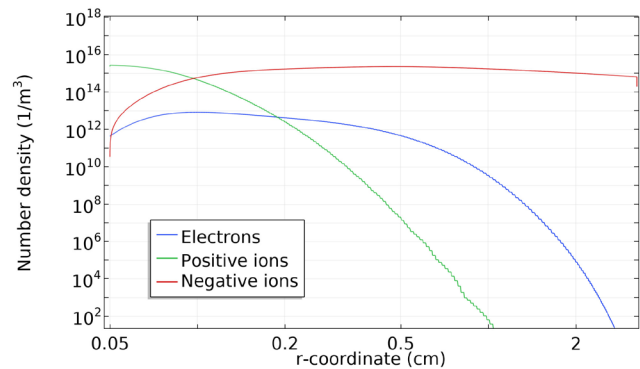


Fig. 2 Negative corona - Charge carriers in logarithmic scale

of negative ions appear in the vicinity of the corona electrode, but it does not last far from the corona electrode. In fact, as it must be expected, a greater number of positive ions are present and remain with almost the same density throughout the space between the electrodes.

In contrast, with the negative corona see Fig. 2, the number of positive ions in the vicinity of the corona electrode is much higher than the number of negative ions and electrons, however, the density of positive ions stays only about some millimeters from the corona electrode. The electron density is high at the corona electrode, but it lasts only some millimeters from the corona electrode. The negative ions are the predominant charge carriers as was expected. The electric potential profile is shown in Fig. 3, it compares the two models introduced previously, the plasma model is more accurate, however, the results obtained from the simplified model show a good approximation.

The space charge density obtained from the two models is shown in Fig. 4. The models for negative corona match their results, however, the models for positive corona do not match accurately, but it trends to the same final value.

The graphs are shown on a logarithmic scale, it is recommended not to interpret the results directly, and part of the discussion is written in a general way.

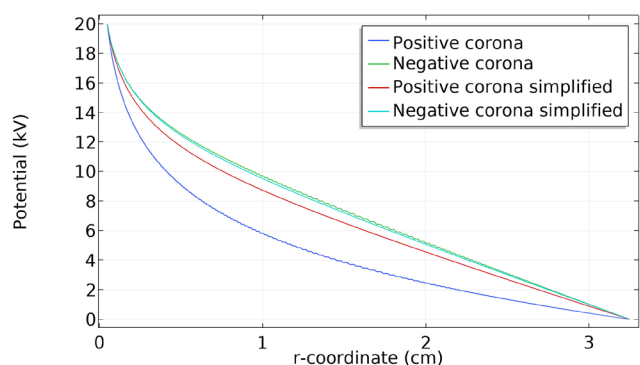


Fig. 3 Electric potential profile obtained from the plasma and simplified model

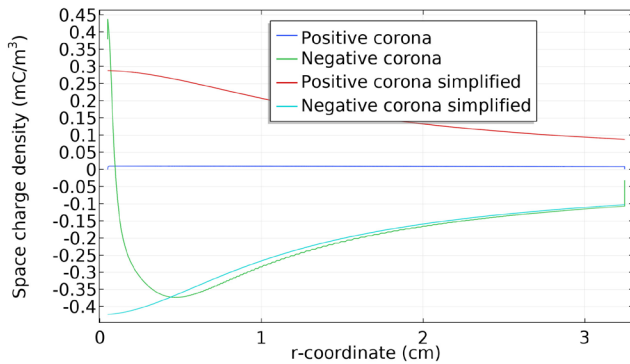


Fig. 4 Negative corona - Charge carriers in logarithmic scale

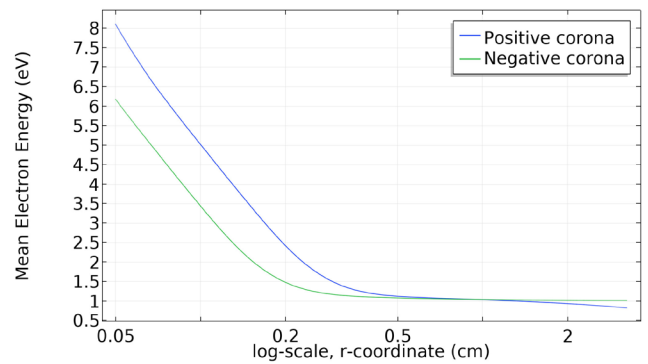


Fig. 6 Electron temperature for a positive and negative corona

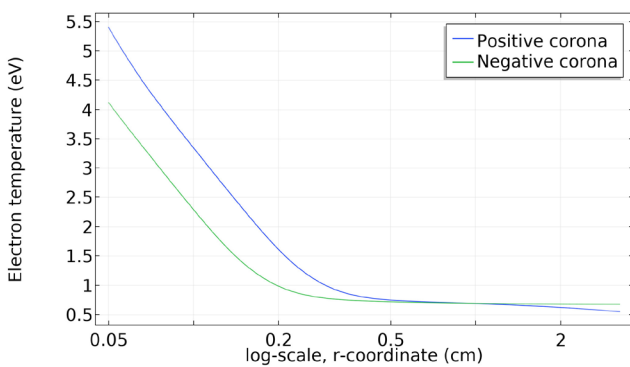


Fig. 5 Electron temperature for a positive and negative corona

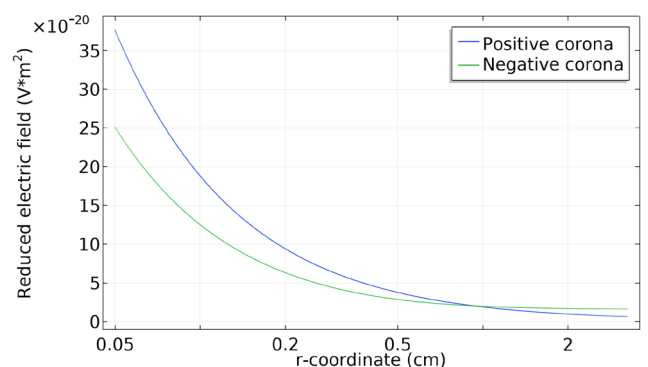


Fig. 7 Reduced electric field for a positive and negative corona

Fig. 5 shows the electron temperature for both coronas obtained from the plasma model results. It seems higher values of temperature are reached for a positive corona than a negative corona. Indeed, the same trend presents the mean electron energy as the electron temperature, see Fig. 6.

The reduced electric field was introduced as part of the plasma model, the results are shown in Fig. 7.

5 Conclusions

A simulation of a specific study case (see Table 2) was carried out using COMSOL; two models are presented as part of the solutions proposed by this software. Following the instructions for the modeling and parameters setting the results for this specific study are presented. The results

obtained are like the ones proposed by COMSOL. Defining a plasma model is a long process to get the results if it is compared with a simplified model. The results of electric potential and space charge density from the two models are similar, but the results from the plasma model can be interpreted as more accurate to a real phenomenon, however, in terms of computational resources a simplified model performs better than the plasma model. Using the plasma model is more expensive in terms of computation, but this model can give a wider description of the carrier carriers.

Acknowledgment

This work is supported by the Stipendium Hungaricum Scholarship.

References

- [1] White, H. J. "Industrial Electrostatic Precipitation", Addison-Wesley Publishing Company, Boston, USA, 1963.
- [2] COMSOL Multiphysics "Positive and Negative Corona Discharges", [pdf] COMSOL, Inc., Available at: https://www.comsol.com/model/download/947921/models.plasma.positive_and_negative_corona_discharges.pdf [Accessed: 29 January 2022]
- [3] COMSOL Multiphysics "Plasma Module User's Guide", [pdf] COMSOL, Inc., Available at: <https://doc.comsol.com/5.3/doc/com.comsol.help.plasma/PlasmaModuleUsersGuide.pdf> [Accessed: 29 January 2022]
- [4] Chen, J., Davidson, J. H. "Electron Density and Energy Distributions in the Positive DC Corona: Interpretation for Corona-Enhanced Chemical Reactions", Plasma Chemistry and Plasma Processing, 22(2), pp. 199–224, 2002. <https://doi.org/10.1023/A:1014851908545>

- [5] Hagelaar, G. J. M., Pitchford, L. C. "Solving the Boltzmann equation to obtain electron transport coefficients and rate coefficients for fluid models", *Plasma Sources Science and Technology*, 14(4), pp. 722–733, 2005.
<https://doi.org/10.1088/0963-0252/14/4/011>
- [6] Liu, X. H., He, W., Yang, F., Wang, H.-Y., Liao, R.-J., Xiao, H.-G. "Numerical simulation and experimental validation of a direct current air corona discharge under atmospheric pressure", *Chinese Physics B*, 21(7), Article No: 075201, 2012.
<https://doi.org/10.1088/1674-1056/21/7/075201>
- [7] Sima, W., Liu, C., Yang, M., Shao, Q., Xu, H., Liu, S. "Plasma model of discharge along a dielectric surface in N_2/O_2 mixtures", *Physics of Plasmas*, 23(6), Article No: 063508, 2016.
<https://doi.org/10.1063/1.4949767>
- [8] Dong, G., Li, Q., Liu, T., Gao, H., Zhang, M. "Finite-element analysis for surface discharge on polyimide insulation in air at atmospheric pressure under pulsed electrical stress", *High Voltage*, 5(2), pp. 166–175, 2020.
<https://doi.org/10.1049/hve.2019.0242>
- [9] Liu, K.-L., Liao, R.-J., Zhao, X.-T. "Numerical Simulation of the Characteristics of Electrons in Bar-plate DC Negative Corona Discharge Based on a Plasma Chemical Model", *Journal of Electrical Engineering and Technology*, 10(4), pp. 1804–1814, 2015.
<https://doi.org/10.5370/JEET.2015.10.4.1804>
- [10] Sima, W., Peng, Q., Yang, Q., Yuan, T., Shi, J. "Study of the Characteristics of a Streamer Discharge in Air Based on a Plasma Chemical Model", *IEEE Transactions on Dielectrics and Electrical Insulation*, 19(2), pp. 660–670, 2012.
<https://doi.org/10.1109/TDEI.2012.6180261>
- [11] Pancheshnyi, S., Nudnova, M., Starikovskii, A. "Development of a cathode-directed streamer discharge in air at different pressures: Experiment and comparison with direct numerical simulation", *Physical Review*, 71(1), Article No: 016407, 2005.
<https://doi.org/10.1103/PhysRevE.71.016407>
- [12] Potrymai, E. Perstnov, I. "Time Dependent Modelling and Simulation of the Corona Discharge in Electrostatic Precipitators", [pdf] Linnaeus University, Available at: <http://www.diva-portal.org/smash/get/diva2:707884/FULLTEXT01.pdf> [Accessed: 29 January 2022]
- [13] Donkó, Z., Derzsi, A., Vass, M., Horváth, B., Wilczek, S., Hartmann, B., Hartmann, P. "eduPIC: an introductory particle based code for radio-frequency plasma simulation", *Plasma Sources Science and Technology*, 30(9), Article No: 095017, 2021.
<https://doi.org/10.1088/1361-6595/ac0b55>
- [14] Iváncsy, T., Suda, J. M. "Behavior of polydisperse dust in electrostatic precipitators", *Journal of Electrostatics*, 63(6–10), pp. 923–927, 2005.
<https://doi.org/10.1016/j.elstat.2005.03.062>
- [15] Kiss, I., Iváncsy, T., Berta, I. "Precipitation of Fine Particles Considering Uncertain Dust Properties", In: *Proceedings of the IXth International Conference on Electrostatic Precipitation*, Kruger Gate, South Africa, 2004, Article ID: A06.